ISSN 0021-3640, JETP Letters, 2012, Vol. 96, No. 10, pp. 650–654. © Pleiades Publishing, Inc., 2012.
Original Russian Text © M.S. Platunov, S.G. Ovchinnikov, N.V. Kazak, N.B. Ivanova, V.N. Zabluda, E. Weschke, E. Schierle, K.V. Lamonova, 2012, published in Pis'ma v Zhurnal Eksperimental'noi i Teoreticheskoi Fiziki, 2012, Vol. 96, No. 10, pp. 723–727.

Identification of Local Magnetic Contributions in a Co_2FeBO_5 Single Crystal by XMCD Spectroscopy

M. S. Platunov[a, *], S. G. Ovchinnikov[a, b, c], N. V. Kazak[a], N. B. Ivanova[b], V. N. Zabluda[a], E. Weschke[d], E. Schierle[d], and K. V. Lamonova[e]

[a] *Kirensky Institute of Physics, Siberian Branch, Russian Academy of Sciences, Akademgorodok, Krasnoyarsk, 660036 Russia*
** e-mail: platunov@iph.krasn.ru*
[b] *Siberian Federal University, Svobodnyi pr. 79, Krasnoyarsk, 660041 Russia*
[c] *Siberian State Aerospace University, Krasnoyarsk, 660014 Russia*
[d] *BESSY II, Helmholtz-Zentrum, Berlin, 12489 Germany*
[e] *Donetsk Institute for Physics and Engineering, National Academy of Sciences of Ukraine, Donetsk, 83114 Ukraine*

Received October 5, 2012

The temperature dependences of the X-ray absorption spectra (XAS) and of the spectra of X-ray magnetic circular dichroism (XMCD) are measured near the $L_{3,2}$ absorption edges of Co and Fe in ludwigite Co_2FeBO_5 single crystals. The antiparallel orientation of the magnetic moments of cobalt and iron is demonstrated. The coercive fields related to cobalt and iron ions are determined. The orbital (m_l) and (m_s) spin contributions to the total magnetic moments of cobalt and iron ions are identified. The ratios and relative directions of m_l and m_s are found.

DOI: 10.1134/S0021364012220109

1. INTRODUCTION

Oxyborates described by a general chemical formula $M_2M'BO_5$ (where $M = M^{2+}$ = Ni, Cu, Zn, Co, Fe, Mn, Mg, ...; $M' = M^{3+}$ = Ti, V, Cr, Fe, Co, Ga, ...) have the orthorhombic structure (space group *Pbam*), similar to that of ludwigite. The metal ions occupy four nonequivalent crystallographic positions 1(2*d*)–2(2*a*)–3(4*h*)–4(4*g*) and are surrounded by oxygen octahedra [1]. Face-sharing octahedra form zigzag chains directed along the [001] crystallographic axis. There are only two kinds of ludwigite with the same metal ions ($M = M'$), namely, Fe_3BO_5 and Co_3BO_5, with quite different magnetic properties.

Ludwigite Fe_3BO_5 is the most well-studied compound. It exhibits an extremely complicated magnetic behavior. The studies of X-ray diffraction, magnetization, specific heat, electrical resistance, and the Mössbauer effect reveal a series of phase transitions. Two of them are magnetic phase transitions (with $T_{N1} = 115$ K and $T_{N2} = 70$ K). The structural transition at 283 K is accompanied by charge ordering [2, 3]. According to the neutron diffraction data [4], the magnetic moments of iron ions at positions 4–2–4 and 3–1–3 become ordered in the orthogonal manner at T_{N1} and T_{N2}, respectively.

Ludwigite Co_3BO_5 behaves as a three-dimensional ferrimagnet with $T_N = 42$ K. Rather unexpected magnetic properties are found when iron ions are substituted for some cobalt ions. For example, the studies of $Co_{3-x}Fe_xBO_5$ single crystals (with $x = 0.75$ and 1) demonstrated that their magnetic characteristics are closer to those of Fe_3BO_5 rather than to Co_3BO_5 [1, 5]. Both iron-containing materials have a clearly pronounced uniaxial anisotropy and exhibit two magnetic phase transitions at 110 and 70 K. The introduced iron ions induce a drastic increase in the coercivity along the [010] axis as compared to the initial composition Co_3BO_5 [1]. A complicated picture of magnetic interactions resulting from the substitution of iron for cobalt is currently far from being well understood. The role of iron ions in the formation of the magnetic order is still under discussion.

This work is aimed at the study of the contributions to the total magnetization introduced separately by cobalt and iron. As a main method, we used X-ray absorption spectroscopy sensitive to the elemental composition (X-ray beams were generated by a synchrotron radiation source).

As far as we know, no experimental studies of transition metal oxyborates by X-ray absorption spectroscopy (XAS) and through the use of X-ray magnetic circular dichroism (XMCD) have been undertaken up to now. There are also no theoretical and experimental papers treating the local magnetic structure of these materials and its evolution under the effect of applied fields. Therefore, the studies of the local magnetism at the $L_{3,2}$ absorption edges of 3*d* elements in Co_2FeBO_5 ludwigite single crystals near the magnetic transition temperatures are of apparent interest.

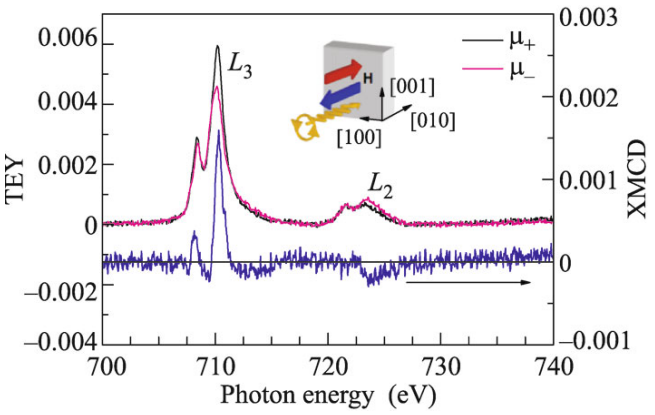

Fig. 1. XAS and XMCD spectra for $L_{2,3}$ edges of Fe, $T = 5$K.

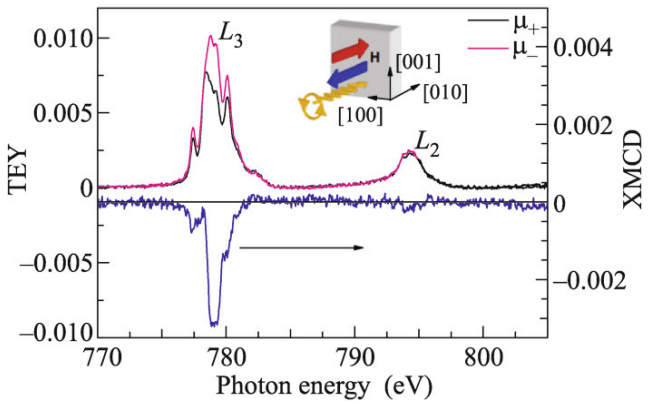

Fig. 2. XAS and XMCD spectra for $L_{2,3}$ edges of Co, $T = 5$K.

2. SAMPLES AND EXPERIMENTAL TECHNIQUES

High-quality Co_2FeBO_5 single crystals were grown by the spontaneous crystallization from the solution melt ($a = 9.3818$ Å, $b = 12.3445$ Å, and $c = 3.0578$ Å). The detailed description of the growth technique is given in [1]. The grown single crystals have the shape of platelets with the typical sizes of $1.5 \times 0.25 \times 4$ mm. The long and short sides of such platelet coincide with the [001] and [010] crystallographic directions, respectively.

The measurements of X-ray absorption spectra (XAS) at the $L_{3,2}$ absorption edges of cobalt and iron were performed at the special-purpose UE46-PGM1 beamline at the BESSY II synchrotron (Helmholtz-Zentrum, Berlin, Germany). The polarized radiation was generated by a helical undulator. We used a PGM plane grating monochromator. The measurements were taken at an applied magnetic field up to 60 kOe generated by the superconducting magnet within the 5–130 K temperature range. The spectra were recorded using the total electron yield (TEY) mode by measuring the electric current flowing from the sample. The XMCD was determined as the difference $\mu_{XMCD} = \mu_+ - \mu_-$, where μ_+ and μ_- are the coefficients characterizing the absorption of X-rays with the right and left circular polarizations, respectively. According to the dc magnetization measurements, the [010] direction corresponds to the easy magnetization axis. The ferromagnetic magnetization is assumed to be directed along this axis [1]. Therefore, the geometry of experiment was chosen in such a way that the directions of the applied magnetic field and the incident radiation coincided with the [010] crystallographic axis. The processing of experimental data was performed taking into account the self-absorption effect.

3. EXPERIMENTAL RESULTS AND THEIR DISCUSSION

In Figs. 1 and 2, we demonstrate the normalized XAS and XMCD spectra measured for the Co_2FeBO_5 single crystal at 5 K in the applied magnetic field $H =$ 60 kOe. The spectra exhibit a complicated multiplet structure. Analyzing the absorption spectra in the soft X-ray range, we can estimate the electron configuration of the transition metal ions. In [7], the results of ab initio calculations are reported for X-ray absorption spectra at the $L_{2,3}$ absorption edges of transition metals in the crystal field of different symmetries. It is demonstrated that the spectral shape depends drastically on the valence state, crystal field magnitude, and spin state of the ion. Taking into account the octahedral surrounding of the metal ions in Co_2FeBO_5, we compared the measured XAS spectra with the theoretical predictions. The best fit occurs if we assume that the Co and Fe ions correspond mainly to the valence states 2+ and 3+, respectively.

The measured spectra for both Co and Fe exhibit a pronounced XMCD signal at the L_3 edge. It is a signature of the spin–orbit interaction in the final states and at the same time of a nonzero orbital magnetic moment (different final $3d$ states manifest themselves at the L_2 and L_3 edges according to the dipole selection rules).

Within the whole temperature range, the value of the XMCD signal for Co is larger than that for Fe. For these two metals, the signs of the effect are opposite, which is an indication of the antiparallel orientation of the magnetic moments of the corresponding ions. With the growth of temperature, the shape of the XMCD spectra for both ions varies only slightly and the signs of the effects remain unchanged.

If the absorbing atom has a spin magnetic moment, the final states undergo exchange splitting and the

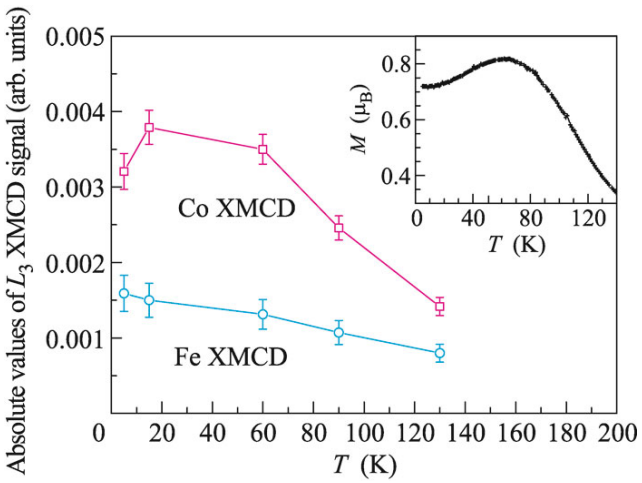

Fig. 3. Temperature dependence of the absolute values of the XMCD signal at the L_3 edge of Co and Fe. The temperature dependence of the magnetization of Co_2FeBO_5 at the applied magnetic field $H = 50$ kOe [1] is shown in the inset.

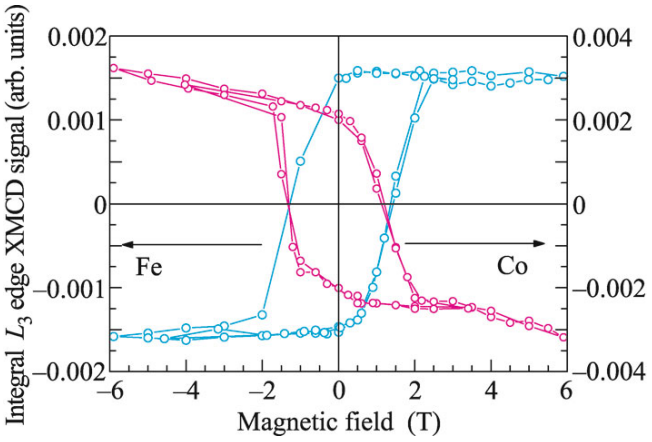

Fig. 4. Element-selective magnetization curves recorded at the L_3 edge of Co and Fe, $T = 5$ K.

XMCD signal turns out to be proportional to the local spin density [8]:

$$\mu_{XMCD} \sim |M(E)|^2[\rho_+(E) - \rho_-(E)], \quad (1)$$

where $M(E)$ is the matrix element of the dipole transition and $\rho_+(E)$ and $\rho_-(E)$ are the densities of the unoccupied states for spin up and spin down, respectively. In Fig. 3, we show the temperature dependence of the XMCD signal at the L_3 edge of Co and Fe. We see that the curves have different forms. For Co, the XMCD signal exhibits a broad peak in the 20–60 K temperature range, whereas the XMCD signal for Fe decreases gradually with an increase in the temperature.

The changes in the intensity of the XMCD signal coming from the given absorbing atom are the indications of the changes in the local magnetization related to Co and Fe. The comparison of the temperature dependence of the XMCD signal and that of dc magnetization (see inset of Fig. 3) shows that the shape of the XMCD signal related to Co qualitatively reproduces the shape of the macroscopic magnetization $M(T)$.

In Fig. 4, we demonstrate the isotherms of the element-selective magnetization measured at the L_3 edges of Co and Fe. The curves have the shape of oppositely directed hysteresis loops. At $T = 5$ K, the Fe sublattice is in the magnetically saturated state. The magnetization related to Co exhibits a clearly pronounced paraprocess suggesting the rotation of the uncompensated magnetic moment toward the applied field direction.

The values of the coercive field H_c turn out to be quite unexpected. The earlier magnetostatic measurements for the bulk samples revealed an unusual growth of the coercivity of Co_2FeBO_5 in comparison to the parent compound Co_3BO_5 [1]. For the applied magnetic field along the [010] crystallographic axis, the coercivity at $T = 15$ K exceeds 90 kOe. Below this temperature, the maximum available applied magnetic field turns out to be insufficient for the remagnetization of the sample. The values of the coercive field determined on the basis of the XMCD studies are much lower. At 5K, they are 12.4 and 13.3 kOe for cobalt and iron, respectively.

Such a difference in the values of coercivity obtained by the bulk measurements and by the surface-sensitive XMCD method can be related to the effect of grain boundaries, noncollinearity of the Co and Fe magnetic subsystems, and characteristic features of the properties of the near-surface Co and Fe ions. Such a difference between the coercive fields measured by XMCD and by the static methods is well known [9, 10]. In our case, the penetration depth of the soft X-ray radiation is of the order of 10 nm, whereas the thickness of the sample under study is about 250 μm.

Important information on the behavior of magnetic subsystems can be deduced by separating out the (m_s) spin and orbital (m_l) magnetic moments.

For transitions from the $2p_{3/2}$ and $2p_{1/2}$ levels to the $3d$ valence band, the ratio of orbital and spin magnetic moments (m_l/m_s) can be determined from XAS and XMCD spectra using the relations [11–13]

$$\frac{m_l}{m_s} = \frac{\langle L_z \rangle}{2\langle S_z \rangle + 7\langle T_z \rangle} = \frac{2\int\limits_{L_3+L_2}(\mu_+ - \mu_-)dE}{9\int\limits_{L_3}(\mu_+ - \mu_-)dE - 6\int\limits_{L_3+L_2}(\mu_+ - \mu_-)dE}, \quad (2)$$

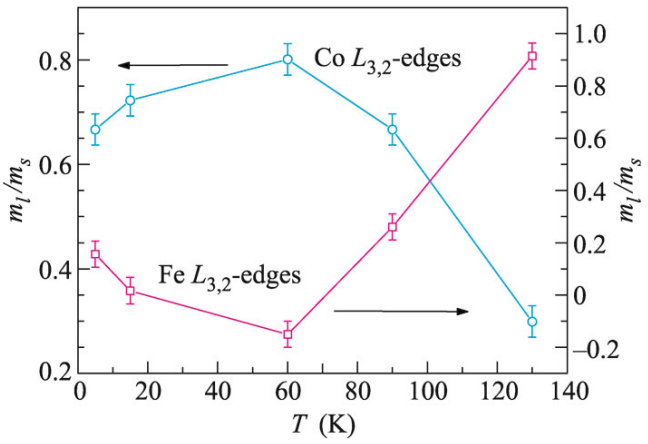

Fig. 5. Temperature dependence of the m_l/m_s ratio for Co and Fe.

where $\langle T_z \rangle$ is the expectation value for the magnetic dipole operator and $\langle S_z \rangle$ and $\langle L_z \rangle$ are the average values of the projections of spin and orbital angular momentum, respectively. Subscripts L_3 and L_2 denote the integral energy range.

Actually, using the sum rules [11, 13], it is possible to determine separately the projections of spin and orbital angular momentum. We give here the data on the m_l/m_s ratio, which can be determined with a higher accuracy than the projections themselves. The calculation of the ratio of two contributions, m_l/m_s, allows avoiding some systematic errors (insufficient accuracy in the number n_{3d} of unoccupied 3*d* states; separating out the contribution of photoelectron excitation to the continuum states; taking into account the anisotropy of the spin density $\langle T_z \rangle$ and radial matrix element independent of energy).

The temperature dependences of the m_l/m_s ratio determined for cobalt and iron in the Co_2FeBO_5 sample are shown in Fig. 5. The values of the m_l/m_s ratio agree with the data obtained in the studies of the Co- and Fe-based magnetic films and alloys [11, 13, 14]. The temperature dependence of m_l/m_s for both metals is nonmonotonic, exhibiting a peak near 60 K. Such a complicated behavior was observed earlier in the studies of Co_N nanostructures [15]. The observed nonmonotonic temperature dependence of m_l/m_s correlates well with the value $T_{N2} = 70$ K known from the static measurements.

Within the framework of the modified crystal field theory [16], we calculated the effective *g* factors and reproduced the components of the *g* tensor for Co^{2+} ions in positions 2*d*, 2*a*, and 4*h* and for Fe^{3+} ion in position 4*g* [1]. On the basis of these calculations, we determined the orientations of magnetic moments for Co^{2+} and Fe^{3+} ions (Fig. 6). We can see that the magnetic moments of Fe^{3+} lie in the direction close to

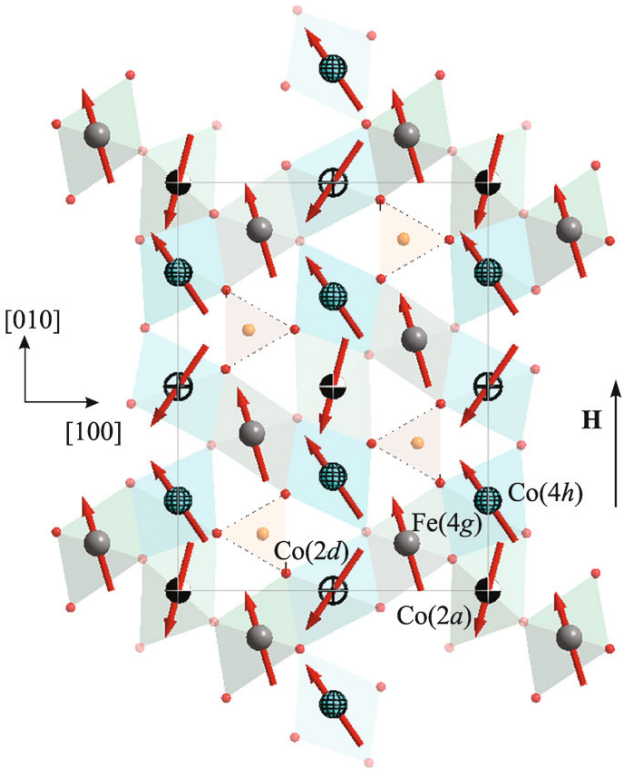

Fig. 6. Directions of the magnetic moments of Co and Fe for each position.

[010]. The magnetic subsystem of Co^{2+} is noncollinear. It is described by three sublattices with a pronounced magnetic bias along the [010] bias due to the Dzyaloshinskii–Moriya interaction. The characteristic features of magnetic structure underlie the observed behavior of the hysteresis loops (see Fig. 4): in the applied field directed along the [010] axis, the magnetization related to Fe^{3+} already achieves saturation at $H = 20$ kOe, whereas the cobalt subsystem does not achieve saturation even at $H = 80$ kOe. The results of the symmetry analysis performed for the magnetic structure of Co_2FeBO_5 agree well with the above conclusions.

Thus, in this work, we have measured the temperature dependence of the XAS and XMCD spectra for the Co_2FeBO_5 single crystal in the soft X-ray range. The electron configuration of Co and Fe ions has been determined. The ratio of the orbital and spin contributions to the total magnetic moment has been found. Their variation with temperature has been studied. We have found the antiparallel orientation of magnetic moments of Co and Fe in the [010] direction. For iron, we have the ferromagnetic ordering of the magnetic moments. This is suggested by the shape of element-sensitive hysteresis loops and by the temperature dependence of the XMCD signal. The magnetic moments of Co ions are antiferromagnetically coupled and have an uncompensated magnetic moment in the

[010] direction (ferrimagnetic coupling). Due to the Dzyaloshinskii–Moriya interaction, the magnetic sublattices become canted and the components of magnetic moments along the [100] axis arise. The XMCD signal at the L_3 edge of Co qualitatively reproduces the temperature dependence of the total magnetization. We have found the coercive fields in the magnetic systems of Co and Fe.

Probably, the magnetic structure of Co_2FeBO_3 is more complicated than was assumed earlier [1]. For further advances in the understanding of this problem, we need additional temperature-dependent studies along different crystallographic axes using XMCD spectroscopy, magnetic X-ray scattering, and neutron diffraction.

We are grateful to L.N. Bezmaternykh for the samples provided for this study and to I.S. Edelman and A. Rogalev for useful discussions. This work was supported by the Russian Foundation for Basic Research (project nos. 12-02-00175-a, 12-02-90410-Ukr-a, and 12-02-31543-mol-a); by the Council of the President of the Russian Federation for Support of Young Scientists and Leading Scientific Schools (project no. NSh-1044.2012.2); by the Siberian Branch, Russian Academy of Sciences (program no. 38); and by the Ministry of Education and Science of the Russian Federation (federal program "Human Capital for Science and Education in Innovative Russia" for 2009–2013).

REFERENCES

1. N. B. Ivanova, N. V. Kazak, Yu. V. Knyazev, et al., J. Exp. Theor. Phys. **113**, 1015 (2011).
2. M. Mir, R. B. Guimaraes, J. C. Fernandes, et al., Phys. Rev. Lett. **87**, 147201 (2001).
3. J. J. Larrea, D. R. Sanchez, F. J. Litterst, et al., Hyperfine Inter. **161**, 237 (2005).
4. F. Borget and E. Suard, Phys. Rev. B **79**, 144408 (2009).
5. J. Bartolome, A. Arauzo, N. V. Kazak, et al., Phys. Rev. B **83**, 144426 (2011).
6. J. Stohr, *NEXAFS Spectroscopy*, 2nd ed. (Springer, Berlin, 1992).
7. G. van der Laan and I. W. Kirkman, J. Phys.: Condens. Matter **4**, 4189 (1992).
8. S. G. Ovchinnikov, Phys. Usp. **42**, 779 (1999).
9. D. R. Lee, Y. Choi, C.-Y. You, et al., Appl. Phys. Lett. **81**, 4997 (2002).
10. D. Haskel, Y. Choi, D. R. Lee, et al., J. Appl. Phys. **93**, 6507 (2003).
11. B. T. Thole, P. Carra, F. Sette, et al., Phys. Rev. Lett. **68**, 1943 (1992).
12. P. Kuiper, B. G. Searle, P. Rudolf, et al., Phys. Rev. Lett. **70**, 1549 (1993).
13. P. Carra, B. T. Thole, M. Altarelli, et al., Phys. Rev. Lett. **70**, 694 (1993).
14. W. L. O'Brien, B. P. Tonner, G. R. Harp, et al., J. Appl. Phys. **76**, 6462 (1994).
15. S. Peredkov, M. Neeb, W. Eberhardt, et al., Phys. Rev. Lett. **107**, 233401 (2011).
16. K. V. Lamonova, E. S. Zhitlukhina, R. Yu. Babkin, et al., J. Phys. Chem. A **115**, 13596 (2011).

Translated by K. Kugel